

- McBurney and J. L. Barker, *Nature (London)* **274**, 596 (1978).
6. H. Korn and D. S. Faber, *Science* **194**, 1166 (1976).
7. D. S. Faber and H. Korn, in *Neurobiology of the Mauthner Cell*, D. S. Faber and H. Korn, Eds. (Raven, New York, 1973), p. 47.
8. E. J. Furshpan and T. Furukawa, *J. Neurophysiol.* **25**, 732 (1962).
9. H. Korn and D. S. Faber, *ibid.* **38**, 452 (1973).
10. D. S. Faber and H. Korn, *Science* **179**, 577 (1973).
11. T. Furukawa and E. J. Furshpan, *J. Neurophysiol.* **26**, 140 (1963); Y. Asada, *Jpn. J. Physiol.* **13**, 583 (1963).
12. Y. Fukami, T. Furukawa, Y. Asada, *J. Gen. Physiol.* **48**, 581 (1965).
13. J. Diamond, *J. Physiol. (London)* **194**, 669 (1968).
14. \_\_\_\_\_, S. Roper, G. Yasargil, *ibid.* **232**, 87 (1973).
15. F. A. Henn, *J. Neurosci. Res.* **2**, 271 (1976); T. Hokfelt and Å. Ljungdahl, *Brain Res.* **32**, 189 (1971); G. A. R. Johnston and L. L. Iversen, *J. Neurochem.* **18**, 1951 (1971).
16. Supported in part by NIH grant NS 12132, INSERM grant CRL 78.5.006.6, and a Ralph Hochstetter Medical Research Advance Award to H.K. in honor of H. C. Buswell and B. H. Buswell. We thank R. Mowry for computer programming, J. R. Teilhac for preparing the figures, and J. Jordan for typing the manuscript.

19 December 1979

## A Disparity Gradient Limit for Binocular Fusion

**Abstract.** *Ever since Panum, it has been commonly assumed that there is an absolute disparity limit for binocular fusion. It is now found that nearby objects modify this disparity limit. This result sheds new light on several enigmatic phenomena in stereopsis.*

It is generally assumed that a stereoscopically presented object will appear fused and single if its binocular disparity falls within Panum's fusional area ( $I$ ). When the disparity exceeds this limit, the object will appear double. An object's disparity may be measured relative to the vergence angle of the eyes or relative to another object in the visual field, such as a fixation point. According to the traditional view, the magnitude of this disparity (or disparity difference) is the critical parameter for fusion.

We find, however, that the disparity gradient rather than the disparity magnitude is the limiting factor for fusion when two or more objects occur near one another in the visual field. The disparity gradient is defined between nearby objects as the difference in their disparities divided by their separation in visual angle. Fusion of at least one object fails when this gradient exceeds a critical value (approximately 1).

To illustrate an implication of the disparity gradient constraint, consider two objects that are moved toward one another in the visual field, while the distances of the objects from an observer are held constant. The disparity gradient between the objects will increase in inverse proportion to object separation and must eventually exceed the gradient limit for fusion. Thus, each object may appear single when the two are widely separated, but when their angular separation becomes sufficiently small, singleness of one or both will necessarily give way to diplopia. This is true even for objects with very small disparities well within Panum's fusional limit.

The minimal stereogram in which the disparity gradient may influence fusion is composed of just two dots. The impor-

tant geometric parameters of the stereogram are the dot separations,  $R_\ell$ ,  $R_r$ , and orientations  $\Theta_\ell$ ,  $\Theta_r$ , in the left and right half-images (Fig. 1A). The binocular dot separation,  $R_b$ , and orientation,  $\Theta_b$ , are defined by the midpoints between the half-images of each dot in the binocular view (Fig. 1B).

The binocular disparity difference of the stereogram is defined as the difference between the individual dot disparities.

$$d_b = d_1 - d_2 = R_r \cos \Theta_r - R_\ell \cos \Theta_\ell$$

The disparity gradient for these dots may be defined as their binocular disparity difference divided by the binocular dot separation,  $d_b/R_b$ . It should be noted that

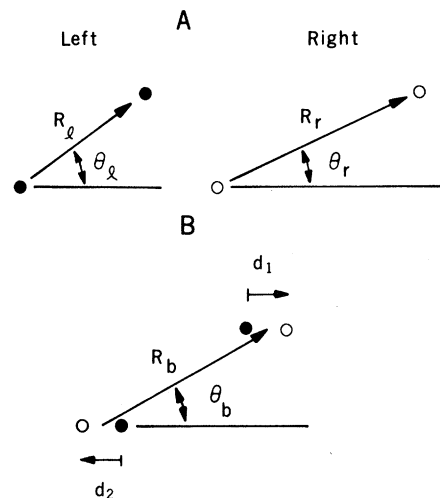


Fig. 1. Geometry of a two-dot stereogram. (A) The half images shown to each eye and (B) the physical pattern after binocular combination. There is no vertical disparity, so  $R_\ell \sin \Theta_\ell = R_r \sin \Theta_r$ . Dots seen by the left eye are shown as filled symbols and dots seen by the right eye as open symbols. In the stereograms these dots are identical.

$R_b$ ,  $\Theta_b$ ,  $d_b$ , and the disparity gradient depend only on stereogram geometry, and are independent of ocular vergence.

When the stereogram is binocularly combined (Fig. 1B), the upper and lower dots may appear at different depths, and their half images may appear fused (single) or diplopic (double). Diplopia occurs when disparities  $d_1$  and  $d_2$  are large. We find that it also occurs for small  $d_1$  and  $d_2$  when  $R_b$  is small.

A new type of stereogram was devised for this study, in which the same periodic image is presented to both eyes (Fig. 2B), and depth results from the "wallpaper" effect. Each "wallpaper stereogram" contains many dot pairs of the type shown in Fig. 1 arranged in a regular array. All pairs have the same disparity,  $d_b$ , and orientation,  $\Theta_b$ . In addition, all pairs within a row have the same separation,  $R_b$ . However,  $R_b$  is increased from row to row as one moves up the stereogram. Thus the disparity gradient,  $d_b/R_b$ , changes systematically over the stereogram.

For an initial experiment, separate stereograms were constructed for each of four angles,  $\Theta_b$ , and four disparities,  $d_b$ . A range of  $R_b$  was chosen for each stereogram so that fusion was obtained near the top and diplopia near the bottom. Stereograms were drawn on a hard-copy unit (Tektronix 4631) and measured 15 by 20 cm each.

Three subjects viewed the stereograms from 50 cm and reported the number of the row that appeared to fall at the boundary between regions of fusion and diplopia, the row at which fusion and diplopia seemed equally likely to occur.

In a second experiment, the viewing distance was varied in order to extend the range of disparities studied. A set of 15 stereograms differing in disparity but not in orientation ( $\Theta_b = 90$ ) were viewed from three distances (25, 50, and 100 cm).

Fusion was not always obtained above the reported transition row, and scrutiny of dots often caused diplopia. Diplopia always occurred below the reported transition row.

The dot separation,  $R_b$ , was determined for each of the rows reported by subjects in three observations of a stereogram. These were averaged to obtain a single estimate of the critical dot separation,  $\hat{R}_b$ , which marked the boundary between fusion and diplopia. Transition values for one observer are shown in Fig. 3 as a function of  $d_b$ . Separate curves have been drawn in Fig. 3A for each angle  $\Theta_b$  and in Fig. 3B for each viewing distance.

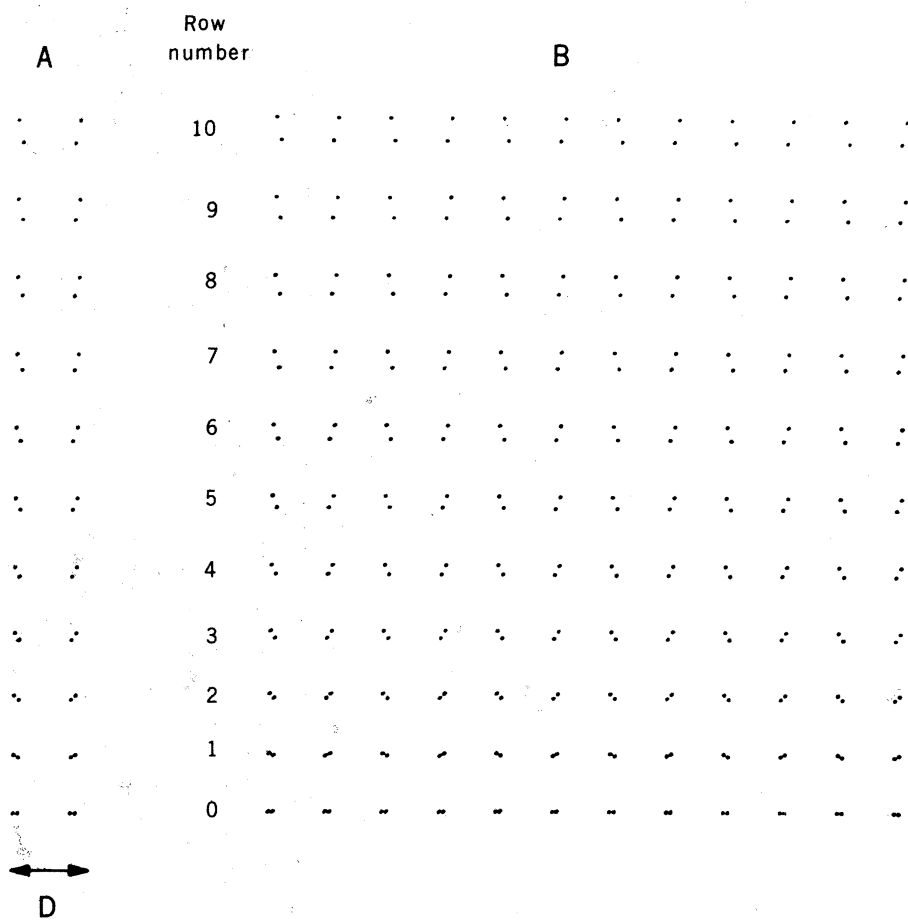


Fig. 2. A wallpaper stereogram. A typical stereogram is constructed by arranging the left and right halves of a number of two-dot stereo pairs in vertically oriented columns. The columns are placed side by side and are separated by a distance  $D$  (A). These two columns are then copied at regular horizontal intervals,  $2D$  (B). The wallpaper stereogram should be viewed by either crossing or diverging the eyes slightly, so that neighboring columns are binocularly superimposed. The two dots of each pair are then seen at different depths. The separation of columns and rows is sufficiently large that the dot interactions critical to fusion occur only within pairs. Our subjects reported fusion above row 5 of this particular stereogram and diplopia below, independent of overall scale (viewing distance).

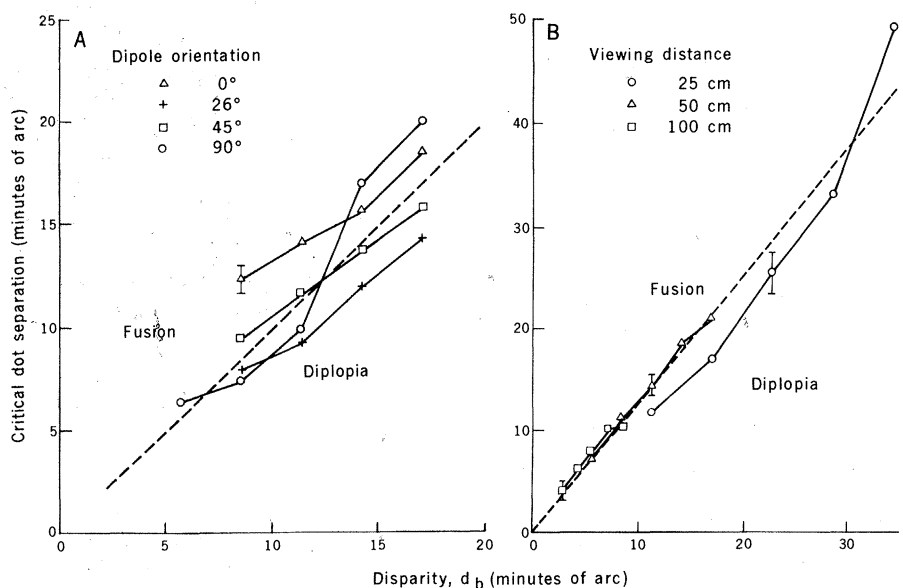


Fig. 3. Critical dot separations as a function of disparity and orientation. Observed  $\hat{R}_b$  are shown for various values of disparity,  $d_b$ . In (A), separate symbols indicate data obtained for four  $\Theta_b$  orientations, 0, 26, 45, and 90 degrees. In (B), symbols indicate data obtained at three viewing distances, 25, 50, and 100 cm.  $\Theta_b = 90$  degrees.

Dot disparity played a critical role in determining the limiting dot separation for fusion: each curve for each observer increased approximately linearly with  $d_b$ . This empirical relationship may be approximated by the equation:

$$\hat{R}_b = k d_b \quad (1)$$

The dashed lines in Fig. 3 indicate the least-square error fits of Eq. 1 to data for all  $d_b$  and  $\Theta_b$  in experiment 1 and for all viewing distances in experiment 2. Deviation of data from these curves may be due in part to the choice of test stereograms. Relatively large row-to-row changes in  $R_b$  prevented precise estimates of  $\hat{R}_b$ . The data obtained for the four values of  $\Theta_b$  differ systematically, but this is a secondary effect. The direction of these differences was not consistent across observers, and we conclude that, to a first approximation,  $k$  is independent of orientation,  $\Theta_b$ .

The reciprocal of  $k$  is the ratio  $d_b/\hat{R}_b$  and is an estimate of the critical disparity gradient that marks the boundary between fusion (smaller gradients) and diplopia (larger gradients). The average gradient limit for our observers in the first experiment was  $0.93^\circ \pm 0.05^\circ$  and in the second  $1.04^\circ \pm 0.3^\circ$  disparity per degree of visual angle. The gradient constraint is roughly isotropic with respect to the direction,  $\Theta_b$ , between interacting objects and applies for dot separations between  $4'$  and  $34'$  of arc. At the low end of this range, fusion was lost at  $4'$  disparity, or less than a third of the value reported by Ogle for the width of Panum's area in the fovea (2).

The disparity gradients in a stereogram do not change as the size scale of the stereogram is changed. Thus, our observation that the disparity gradient determines the fusional state implies a disparity scaling rule. If a given stereogram can be fused, any new stereogram obtained simply by scaling the first can also be fused. The converse is not true, however; that is, a scaling principle does not yield a disparity gradient limit. Tyler, who first observed disparity scaling with sinusoidal lines (3), did not find such scaling with square waves (4). Furthermore, he studied only disparity changes along vertical positions (3, 4), whereas the essence of our finding is that the horizontal disparity limit between pairs of dots for fusion is isotropic with respect to the orientation between the dots. Only this extension to all orientations led to the discovery of the disparity gradient limit.

A number of other fusion studies should be reexamined in light of the gra-

dient constraint. For example, the disparity gradient constraint implies that a single image component in one eye cannot be fused at one moment with more than one component in the other eye. Such "multiple fusion" has been suggested as one explanation of depth perceived in Panum's limiting case (5). This stereogram may be constructed by presenting a single dot to one eye and a pair of dots to the other. In the nomenclature of Fig. 1,  $\Theta_r = \Theta_l = R_l = 0$ . Thus,  $d_b = R_r$ ,  $R_b = R_r/2$ , and the gradient  $d_b/R_b = 2$  is roughly twice as large as the limit we observed, so multiple fusion cannot occur.

The disparity gradient limit for fusion also implies that fusion space cannot "fold back" on itself when two or more objects occur at the same vertical level in the visual field. That is, fusion is not possible if the left-to-right order of the object images is reversed in one eye with respect to the other. Simple geometry will confirm that in this case,  $d_b/R_b > 2$ , which is outside the bounds for fusion.

We have found that fusion is never obtained when the disparity gradient exceeds a critical value of approximately  $1^\circ$  of disparity per degree of dot separation. Thus, diplopia occurs even for dots with disparities well within the classical Panum's fusional area whenever the gradient limit is exceeded. It is this failure of fusion under normally favorable conditions that most clearly demonstrates the critical role of object interactions in fusion. It seems that nearby objects "warp" the fusional space, creating forbidden zones in which changes in disparity are too steep for fusion.

PETER BURT\*, BELA JULESZ

Bell Laboratories,  
Murray Hill, New Jersey 07974

#### References and Notes

1. K. N. Ogle, *Researches in Binocular Vision* (Saunders, Philadelphia, 1950).
2. Ogle (1) found that fusion was obtained between roughly  $\pm 7'$  of arc disparity near the fovea. Thus, the total width of Panum's fusional area is  $14'$  of arc.
3. C. W. Tyler, *Science* **181**, 276 (1973); *Nature (London)* **251**, 140 (1974).
4. C. W. Tyler [*Vision Res.* **15**, 583 (1975)] has examined fusion when vertical disparity changes across horizontal positions. These results should not be confused with ours, in which the disparities are always horizontal. He also studied vertical line stereograms wiggling sinusoidally or in square-wave fashion and failed to observe disparity scaling for the latter (see his figure 9A).
5. K. N. Ogle [in *The Eye*, H. Davson, Ed. (Academic Press, New York, 1962), vol. 4, p.374] suggested that multiple fusion could account for depth in Panum's limiting case if disparities fall in Panum's fusional area. However, L. Kaufman and B. Lane [*Invest. Ophthalmol. Suppl.* **174** (1979)] argued that depth is due to eye vergence rather than multiple fusion.

\* Present address: Computer Vision Laboratory, Computer Science Center, University of Maryland, College Park 20742.

11 December 1979

## Telemetered Electromyography of Forelimb Muscle Chains in Gibbons (*Hylobates lar*)

**Abstract.** Electromyographic studies of brachiation in the gibbon controvert deductions, based on dissection, about the purported functions of muscle chains in the hylobatid forelimb. Neither force conduction distally along the components of the chains nor simultaneity of muscular contraction occurs in brachiation. Rather, the unique structure of the forelimb is probably the result of evolved changes in the short head of biceps brachii to enhance its role as a forearm flexor.

The acrobatic arm-swinging locomotion (brachiation) and highly specialized forelimb morphology of the lesser apes *Hylobates* (gibbon) and *Symphalangus* (siamang) have fascinated and puzzled natural historians, comparative anatomists, and anthropologists for more than a century (1, 2). Brachiation dominates the locomotor repertoire of all lesser apes (3); and of all primates only these regularly engage in ricocheting brachiation (2-4), wherein the forelimbs act as propellant organs to hurl the animals across gaps in the forest canopy. Among the most prominent structural modifications in hylobatids are two sets of multiple-joint muscles that appear to be fused into two interacting chains: a ven-

tral chain (pectoralis major to short head of biceps brachii to flexor digitorum superficialis) and a dorsal chain (latissimus dorsi to dorsoepitrochlearis to short head of biceps brachii to flexor digitorum superficialis). Deductive speculations about the function of these chains are based on dissection; they can be traced as far back as Sir Arthur Keith in the late 19th century (5), and have continued unabated to the present (6-9).

The ventral chain is purported to conduct the flexor force of the pectoralis major distally across shoulder, elbow, and wrist joints so that active or passive tension in this muscle results in automatic flexion of the forearm and fingers without requiring activity in the distal mem-

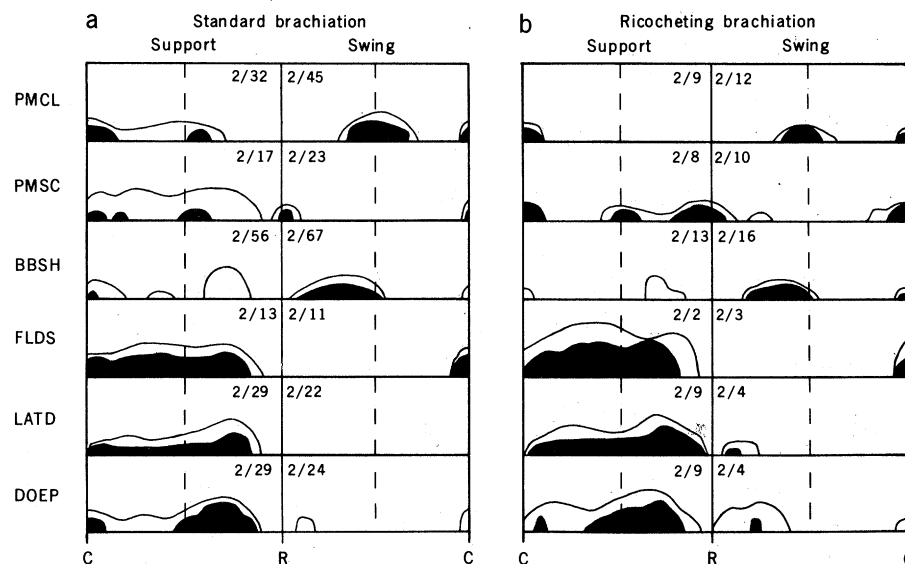


Fig. 1. Muscular activity during standard (a) and ricocheting (b) brachiation in *Hylobates lar*. Muscular components of the chains include pectoralis major pars claviculalis (PMCL), pectoralis major pars sternocostalis (PMSC), short head of biceps brachii (BBSH), flexor digitorum superficialis (FLDS); latissimus dorsi (LATD), and dorsoepitrochlearis (DOEP). Contact and release of the dowels are indicated by C and R, respectively; the dashed lines denote the middle of each phase of brachiation. The first number in each box refers to the number of individuals; the second, to the number of phase cycles counted (10). Blackened regions indicate highly consistent activity occurring at least 67 percent of the time in both animals; enclosed white regions, frequent but not consistent activity occurring at least 67 percent of the time in one subject or 33 percent of the time in both subjects. The height of each blackened or enclosed region indicates the relative amplitude of activity. Activity in a proximal member of the ventral chain (pectoralis major pars sternocostalis) was recorded at the moment of release—as the fingers were extending. Activity observed in proximal elements of the chains during the remainder of the swing phase was not associated with digital flexion. The activity of the flexor digitorum superficialis in the support phase (to establish a stable grip) and of the biceps brachii in the swing phase (to produce elbow flexion and thereby reduce the moment of inertia) demonstrates that, for these purposes, the animal does not rely on force conduction from more proximal muscles.